ORIGINAL PAPER

Biodegradability of blends based on aliphatic polyester and thermoplastic starch

Vesna Ocelić Bulatović[1] · Dajana Kučić Grgić[1] · Miroslav Slouf[2] · Aleksandra Ostafinska[2] · Jiri Dybal[2] ·
Antun Jozinović[3]

Abstract

In this work, biodegradable aliphatic polyester blends of polycaprolactone and polylactide were melted and blended with a natural and biodegradable thermoplastic starch (TPS). The TPS employed in this study was obtained by plasticization of isolated wheat starch using glycerol as plasticizer. Morphology as well as thermal properties of the blends was investigated, and water vapor permeability as a barrier property was also monitored. The biodegradability of the biodegradable blends was performed by a composting process on laboratory scale. The composting process was conducted in an adiabatic closed reactor for 21 days and during the composting process, the temperature, pH value, % moisture and volatile matter and evolved CO_2 were monitored. Biodegradation of the blends was determined by weight loss, as well as monitoring of morphological surface change. The thermophilic phase prevailed in the composting process, indicating intensive biodegradation of substrate as well as biodegradation of investigated ternary blends. Since microorganisms use starch as a carbon source, addition of TPS causes considerable acceleration of biodegradation of ternary blends due to higher water vapor permeability as a result of the hydrophilic nature of starch. The thermoplastic starch was first degraded within the blend, which was facilitated access to the microorganisms of other ingredients in the blend, encouraging the biodegradation of other components.

Keywords Aliphatic polyester · Thermoplastic starch · Biodegradation · Composting process

✉ Vesna Ocelić Bulatović
vocelic@fkit.hr

1   Faculty of Chemical Engineering and Technology, University of Zagreb, Marulićev trg 19, 10 000 Zagreb, Croatia

2   Institute of Macromolecular Chemistry, Academy of Sciences of the Czech Republic, Heyrovsky Sq. 2, 162 06 Prague 6, Czech Republic

3   Faculty of Food Technology, University of Josip Juraj Strossmayer Osijek, F. Kuhača 20 pp 709, 31 000 Osijek, Croatia

Introduction

Non-degradable materials, petrochemical-based plastics such as polyethylene (PE), polypropylene (PP), polystyrene (PS), and polyethylene terephthalate (PET), because of their large availability and enviable properties, have a growing path of use as packaging materials. The use of non-degradable materials as disposable packaging material significantly disturbs and damages the ecosystem (Carmona et al. 2015). They cause irreversible pollution of our environment. Consciousness that our petroleum resources are limited as well as increasing environmental awareness causes limitations of the use of petrochemical plastics, because they pose serious ecological problems and are not be completely recycled and/or biodegraded (Siracusa et al. 2008; Sorrentino et al. 2007; Gumede et al. 2018). Because of that, biodegradable polymers are becoming more and more technologically important as replacement of conventional synthetic polymers for common and specific application, especially as packaging materials. Polylactide (PLA) and polycaprolactone (PCL) are two well-known and most important biodegradable

materials with interesting and complementary properties, which are already remarkable and researched (Labet and Thielemans 2009; Carbonell-Verdu et al. 2018). PLA is an aliphatic hydrophobic biodegradable polyester. Its excellent properties, such as high mechanical performance, point out that it can be used in many applications (Huang 2005; Yu et al. 2006; Palsikowski et al. 2018; Musioł et al. 2018). PLA has a high tensile strength and elastic modulus, but very low elongations at break (Auras et al. 2004; Lu et al. 2017). The expressed brittleness restricts its use as packaging materials. PLA degradation takes place very slowly, especially for unmodified PLA, which according to literature has shown that degradation can take place even after 1 year in seawater (Selke 2000; Auras et al. 2004; Musiol et al. 2018). Degradation of PLA is mainly activated by hydrolysis and is highly dependent on temperature. On the other hand, PCL is another semi-crystalline linear aliphatic biodegradable polyester with high potential to be used as packaging materials (Siracusa et al. 2008; Ortega-Toro et al. 2015; Garcia-Campo et al. 2017; Gumede et al. 2018). PCL has a high elongation and low elastic modulus, which can perfectly complement the defects of the mechanical properties of PLA. Despite the presence of hydrolytically labile aliphatic ester linkages, PCL exhibits a slower hydrolytic degradation rate when compared with PLA (2–3 years) (Nair and Laurencin 2007). Consequently, changing and adapting the properties of these materials is the focus of scientific research. One of the most effective approaches, which is an inexpensive and fast procedure, unlike the development of new polymeric materials or new polymerization, is a blending that combines the best attributes of a particular polymer. Modification of a single biodegradable polymer by blending with other biodegradable materials provides improved and/or maximizes the performance of the material for the targeted purpose. One of the main and very important drawbacks of PCL and PLA is their high cost, which greatly limits their wide commercial use. The alternative to overcome the aforementioned main disadvantage could be blending them with thermoplastic starch (Carmona et al. 2015; Abdul et al. 2017; Antosik and Wilpiszewska 2018; Ortega-Toro et al. 2015). Natural biodegradation in a wide range of environments, low cost and natural abundance in most regions deplete thermoplastic starch for use as raw material for biodegradable polymers. By its nature, starch is not a typical thermoplastic polymeric material. From a chemical point of view, starch is composed of a homopolymer of D-glucose, a predominantly linear polymer with some slight branches amylose (alpha-1,4 links between the linear molecules) and highly branched amylopectin (alpha-1,6 links at the branch points) (Sarazin et al. 2008; Kostakova et al. 2017; Ferreira et al. 2016). Since the melting temperature of pure dry starch is near the starch degradation temperature, natural starch should be modified so that it can be processed by

using conventional synthetic polymeric techniques (Taggort 2004; Ortega-Toro et al. 2015). The transformation of natural starch into thermoplastic-like material is called gelatinization (Fig. 1) and the transformed product is known as thermoplastic starch (TPS). The gelatinization process (Fig. 1) involves the addition of a plasticizer under high pressure and mechanical shear force. The main role of the plasticizer is to destroy the crystalline structure and hydrogen bonding in starch under moderate temperature and thereby allow it to be processed in a similar manner to conventional polymers (Carvalho et al. 2003; Curvelo et al. 2001). Plasticizers get in between the polymer chain and act as lubricants, increasing flexibility and movement. Furthermore, plasticizers decrease the glass and melt temperature of the polymer, leading to more processability of starch (Selke et al. 2004). For the effective gelatinization process of natural starch, it is important that the chemical structure of plasticizers is similar to those of polymers (Huang et al. 2005; Tumwesigye et al. 2016). The most commonly used plasticizers are organic liquid plasticizers, most commonly polyols hydrophilic plasticizers containing hydroxyl groups, such as glycol, sorbitol, sugars, and glycerol. Glycerol is the most popular plasticizer among those listed (Brody 2005; Jiang et al. 2006; Huang et al. 2005). Because of its hydroscopic nature, thermoplastic starch itself is characterized by moisture sensitivity and poor mechanical properties. However, TPS has low oxygen permeability and thus could potentially play an oxygen barrier role in biodegradable packaging. Therefore, blending TPS with PCL/PLA blends can decrease the material cost and increase its biodegradability.
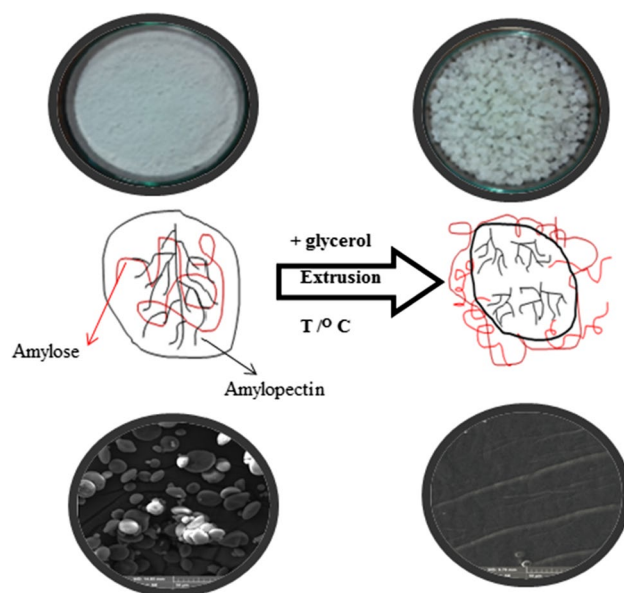

Fig. 1 Gelatinization process of the wheat starch

The objective of this study is the production of the binary and ternary blends with different compositions of PLA, PCL, and 30 wt% of TPS, using the TPS polymer with specifically 30 wt% of glycerol content. Blends are characterized by scanning electron microscopy (morphology); Fourier transform infrared spectroscopy (identification of functional groups); differential scanning calorimetry (thermal properties); water vapor permeability (barrier properties); and biodegradation under composting process (biodegradability). The most important aim of this study is to promote the biodegradation of PLA, PCL polymers and their blends by adding thermoplastic starch.

Experimental

Materials

The wheat variety "Srpanjka" (harvest 2008) was obtained from the Agricultural Institute, Osijek, Croatia. According to the data provided with samples, the "Srpanjka" variety contained 68.73% d.m. starch, 12.57% d.m. protein and 12.20% moisture. Isolation of starch from wheat and characterization of starch were made by our colleagues, as described in their research (Ačkar et al. 2010). The content of amylose in isolated wheat starch was 22.49 ± 2.01 wt%. Glycerol was supplied by Gram Mol (Zagreb, Croatia). Polylactide was supplied by Nature Works LLC, USA (Ingeo™ Biopolymer, 4043D, density 1.24 g cm^{-3} at 25 °C, $T_g = 50$–70 °C, $T_m = 145$–160 °C) and polycaprolactone by Sigma-Aldrich, Germany (polycaprolactone 440744-500G, average M_n 70,000–90,000 g mol^{-1} by GPC, $M_w/M_n < 2$, density 1.145 g cm^{-3} at 25 °C).

Preparation

Thermoplastic starch (TPS) was prepared from a manual mixture of the following components: 70 wt% native wheat starch and 30 wt% glycerol. TPS was extruded with a laboratory single-screw extruder (Model 19/20DN; Brabender GmbH, Germany). The extrusion parameters were as follows: screw 1:1; die 4 mm; temperature profile in the first (dosing), second (compression) and third (ejection) zone 100/100/130 °C; screw speed 40 rpm; dosing speed 15 rpm. After extrusion, the samples were air-dried overnight and then stored in sealed plastic bags at room temperature until further analysis. The binary and ternary blends were prepared using a Brabender kneading chamber. The components were put in the chamber preheated up to 170 °C with a rotor speed of 50 rpm and kneaded for 6 min. After homogenization, the blends were molded in laboratory hydraulic press Fontune, Holland (SRB 140, EC 320x320NB) (180 °C; 25 bar, 5 min). Throughout this paper, the designation,

for example PCL30/PLA70, refers to 30 wt% of PCL and 70 wt% of PLA in the blend. After preparation of the PCL/PLA blends, TPS was then blended with blends in a weight composition of 30 wt% (example PCL50/PLA50/TPS).

Differential scanning calorimetry (DSC)

Thermal analysis was done using a model DSC 823e differential scanning calorimeter (Mettler Toledo, Greifensee, Switzerland) with a quench cooling accessory, operated under a nitrogen atmosphere with flow of nitrogen of 60 ml min^{-1}. All DSC experiments were done in duplicate and the thermograms shown refer to the second heating. DSC measurements were performed according to the following method:

1. Heating up from 0 to 200 °C with a heating rate of 10 °C min^{-1}.
2. Holding on at 200 °C for 2 min to eliminate any previous material thermal history.
3. Cooling with liquid nitrogen from 200 to − 90 °C at 10 °C min^{-1}.
4. Holding on at − 90 °C for 2 min.
5. Second heating from − 90 to 25 °C with a heating rate of 10 °C min^{-1}.

The crystallization and melting parameters were taken from the cooling and reheating scans. The degree of crystallinity, χ_c (%), of both PCL and PLA was determined according to Vertuccio et al. (2009) using Eq. (1):

$$\chi_c \, (\%) = \frac{\Delta H_{exp}}{\Delta H_0 \times f} \times 100, \tag{1}$$

where ΔH_{exp} is fusion enthalpy (J g^{-1}) determined by DSC measurement, ΔH_0 is theoretical enthalpy of the completely crystalline polymer, which is 132 J g^{-1} for PCL (Crescenzi et al. 1972) and 93.7 J g^{-1} for PLA (Chen et al. 2006), and the wt% of PCL or PLA is given by the term f.

Water vapor permeability (WVP)

Water vapor permeability (WVP) of the blends was carried out on the Herfeld's apparatus according to DIN 53333 (Bota et al. 2017). Herfeld's apparatus consists of a glass container that is filled with 50 ml of distilled water and closes with a metal ring which contains a circular hole of diameter 36 mm. The test sample is placed face down on the cover of the vessel of circular diameter 55 mm and tightened with the metal ring. The glass container is placed in a desiccator with 97% sulfuric acid. The weight of the glass container with the test samples and the water is determined at the beginning and after the given time interval of 24 and 48 h. Water vapor

permeability (WVP) is determined according to equation, Eq. (2):

$$WVP = \left[m_0 - (m_2 + m_3)/2\right]/A, \qquad (2)$$

where m_0 is the mass of the device with water and specimen at the beginning (g), m_2 is the mass of the device with water and a test tube after 24 h (g), m_3 is the mass of the device with water and a test tube after 48 h (g), $A = r^2\pi$ is the film surface of the examined sample, and r is the radius of the film permeation area.

Biodegradability test

Composting materials

In this work, mixture of biowaste (BW) and green waste (GW) was used as a composting substrate. Biowaste (vegetable waste, fruit waste and bread) and green waste (leaf and branches) were collected from Dolac Market: Fresh Goodies, Zagreb, Croatia, and in the forest near Zagreb, Croatia, respectively. The pH value and moisture of biowaste were between 4.5 and 6.0 and between 70 and 90%, respectively. The pH value and moisture of green waste was between 5.0 and 6.0 and between 5 and 6%, respectively.

Composting process

The composting of BW and GW was conducted in a closed thermally insulated cylindrical stainless steel reactor ($d = 212$ mm, $h = 330$ mm) with effective volume (V_r) of 10 dm^3 for 21 days. The moisture content of the substrate was set at approximately 60 mass%, pH value was 6.2, C/N ratio 30/1 and 2.5 kg of the mixture was fed into the reactor from the top. The air inlet was placed at the bottom of the reactor and the reactor was operated at an airflow rate of 0.868 dm^3 min^{-1}. The temperature was monitored by thermocouples placed at the reactor's inlet and in the middle of the reactor and connected to the data logger over the 21 days of composting. To ensure permanent air humidity at the reactor's inlet, the air was saturated with moisture prior to entering the reactor by passing through a Drechsel bottle. After leaving the reactor, the hot spent air was allowed to cool naturally and the condensate was collected in the graduated cylinder. In the composting process, 11 polymer blends was added. Two pieces of each polymer/blend ($A = 1$ cm^2) were mixed with the composting substrate.

During the composting process, samples of composting material (without polymer) were collected periodically and the most relevant physical–chemical (pH value, moisture content (MC), dry solid content (DS), volatile solids content (VS), N content (according to Kjeldahl method)) and microbiological characteristics were determined. All physical–chemical analyses were carried out in duplicate and

in accordance with the Austrian standard methods for the analysis of compost, which are in widespread use across Europe (Austrian standard 1986). Colony-forming units (CFU) of mesophilic and thermophilic bacteria and fungi were determined on the general-purpose media (nutrient agar for bacteria and malt agar for fungi) by the pour plate method (Briški et al. 2012). For the plate count, a dilution series (0.9% mass of aqueous NaCl solution) was prepared from each sample. The plates were incubated in 80% relative humidity at 28 °C to cultivate the mesophilic fungi, at 37 °C to cultivate the mesophilic bacteria and at 50 °C to cultivate the thermophilic microorganisms. To determine the concentrations of the evolved CO_2, the exhaust gas was absorbed in 1 mol dm^{-3} NaOH. CO_2 was analyzed daily by titration of the excess of 1 mol dm^{-3} NaOH with 1 mol dm^{-3} HCl (Kolthoff and Sandel 1951). The results were expressed as g CO_2 per kg of the dry composting mass.

Scanning electron microscopy (SEM)

Morphological characterization of selected samples was done by means of scanning electron microscopy (SEM) using a microscope Vega Plus TS 5135 (Tescan, Czech Republic) with a secondary electron imaging (SE) at 30 kV. The samples were observed both before and after degradation tests. For each sample, two types of specimens were prepared for microscopic characterization: top surface and fracture surface. The top surfaces were observed directly. The fracture surfaces were prepared in liquid nitrogen perpendicular to the surface. All specimens were fixed on a metallic support to minimize charging: the flat specimens showing top surfaces were fixed with double adhesive conductive carbon tape (C-tape; Christine Gropl, Austria), while the fracture surfaces were fixed with a conductive silver paste (Leitsilber G302; Christine Groepl, Austria). For further minimization of charging and sample damage by the electron beam, all specimens were sputtered with a thin Pt layer (ca 8 nm) in a vacuum sputter coater (SCD 050; Balzers, Lichtenstein).

Infrared spectroscopy

Attenuated total reflectance (ATR) FTIR spectra were measured on a Nicolet Nexus 870 spectrometer. For all samples, we measured the top surfaces before and after degradation using a horizontal micro-ATR Golden Gate unit (SPECAC) with a diamond prism. The ATR FTIR spectra were processed by the advanced ATR correction using the OMNIC software.

Results and discussion

Thermal properties

Thermal behavior with respect to the thermal transitions of the blends is useful in detecting possible interactions (miscibility behavior) between polymers in binary and ternary blends. The two DSC scan cycles were performed in this investigations. With the first scanning was erased the thermal history of the materials and DSC curves of the second run by scanning from -90 to 200 °C of the materials are shown in Figs. 2, 3 and 4. Table 1 shows a summary of the thermal properties obtained from the DSC thermograms. From Table 1, the glass transition temperature of PLA is at 56.7 °C, which is very close to the melting temperature of PCL at 58.6 °C. Due to the proximity of thermal transition, which leads to some overlapping procedures, it is not possible to clearly distinguish precisely certain thermal transitions of each polymer in the blends. On the other

hand, the glass transition temperature of PCL (T_{gPCL}) was difficult to identify in the resulting DSC curves, due to the limitation of the DSC instrument (possibility of cooling to -90 °C). From the DSC thermogram of PLA, cold crystallization of PLA is observed in the range of 120–135 °C with a peak (T_{ccPLA}) at 127 °C. The cold crystallization is an exothermic peak just before T_{mPLA} of the PLA phase, attributed to the recrystallization of crystals of PLA's lower perfection into α crystals of greater perfection (Feng and Ye 2011). After the cold crystallization process, the melt process follows at a temperature range from 145 to 165 °C with a peak (T_{mPLA}) at 149.4 °C. From the DSC thermogram of PCL, an exothermic melt process is located between 45 and 65 °C with a peak at 58.6 °C, whereas the glass transition temperature of PCL is at -62.8 °C. T_{mPLA} does not change with the addition of PCL at values around 149 °C, but in the blend of the same ratio of both components, PCL50/PLA50, the melting temperature reduction of both, PLA and PCL, components was recorded. By the addition and increase in the content of PCL in PLA, cold

Fig. 2 DSC heating thermograms of PLA, PCL, PLA/TPS, PCL/TPS, PCL50/PLA50 and PCL50/PLA50/TPS
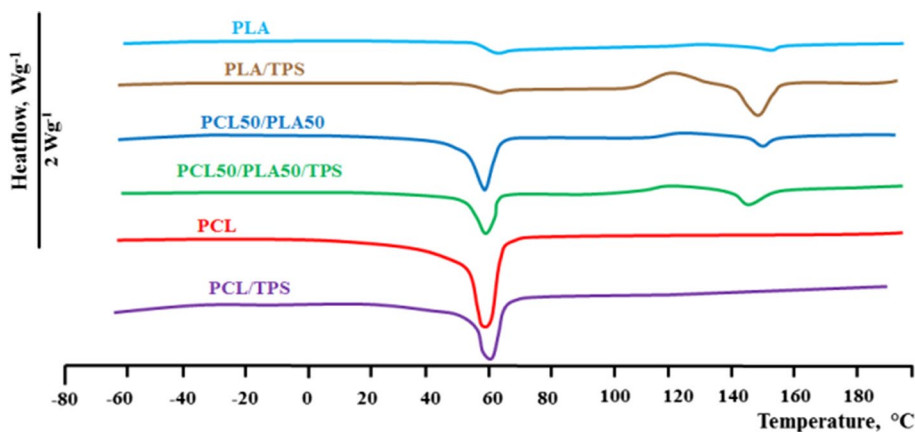

Fig. 3 DSC cooling thermograms of PLA, PCL, PLA/TPS, PCL/TPS, PCL50/PLA50 and PCL50/PLA50/TPS
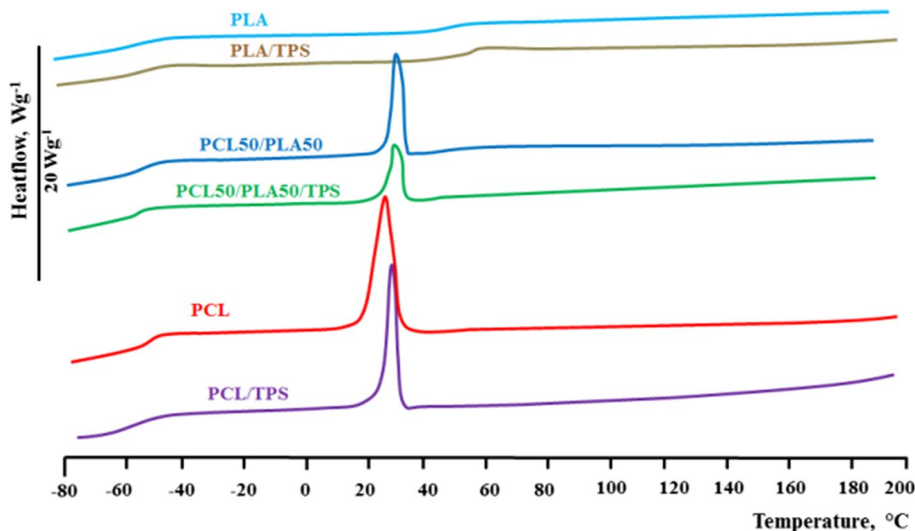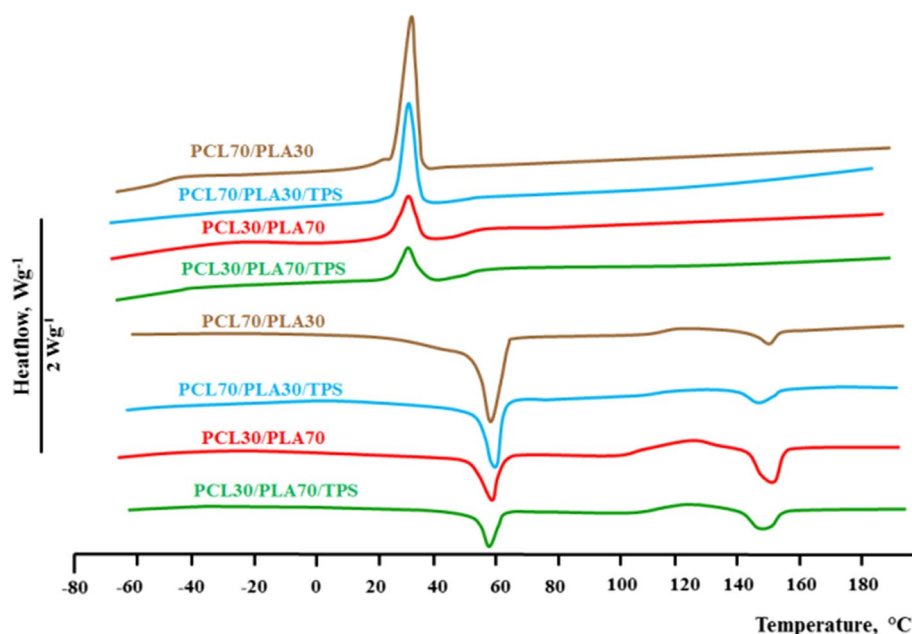
Fig. 4 DSC heating and cooling thermograms of binary and ternary blends

crystallization peak of PLA is slightly shifted to lower temperatures, while on the other hand the addition of PLA to PCL leads to the shift in T_{cPCL} to higher temperatures without significant influence with further increase of PLA content in the blends. However, the degree of PLA crystallinity (χ_{cPCL}) significantly increases with a PCL content compared with pure PLA. Further increase of PCL content, or the same proportion of both components, leads at a lower degree of crystallinity compared to the smaller PCL content in the blend. Probably, the higher content of PCL limits and does not allow the growth of PLA spherulite, which is reflected in the degree of crystallinity. The excess PCL can block or limit the molecular motion of PLA chains and interrupt the growth of PLA spherulites (Ferri et al. 2016). The PLA melting peak, which is very small in pure PLA, is more pronounced in blends. As shown in Fig. 2 and Table 1, the PLA melting peak indicates a shift to lower temperatures with the addition of TPS. This depression in T_{mPLA} is characteristic when a semi-crystalline component (PLA) is miscible with an amorphous polymer such as TPS in these investigated systems. Despite moderate depression, it can be said that a certain degree of miscibility between the components of the blend was achieved. The addition of the TPS in PCL also shows a similar decrease in the PCL melting peak. In general, according to literature, the reduction of the melting peak in a polymer blend is attributed to the morphological effect and reduced lamellar thickness, respectively (Mittal et al. 2015). Also, from the thermodynamics point of view, the reduction of melting peak is associated with a reduction in the chemical potential of the crystallizable polymer due to the presence of the partially miscible amorphous polymer

(Mittal et al. 2015; Broz et al. 2003; Thakur and Thakur 2016). From the DSC heating curve (Fig. 2), it is apparent that TPS contributes to the acceleration of cold crystallization of PLA, where a successive increase in enthalpy of cold crystallization or the degree of PLA crystallinity is clearly seen (Table 1). According to Carmona et al. (2015), TPS can act as a filler and have the role of a nucleating agent, which stimulates PLA cold crystallization and gives a more accurate alignment of polylactide chains in the crystal structure, i.e., influences the significant increase in the degree of PLA crystallinity. From the DSC cooling curve for PLA as well as for PLA/TPS (Fig. 2), there are no visible crystallization peaks during cooling due to the almost amorphous structure of PLA; probably, small crystal phases that are present in the structure are crystallized during cold crystallization. Also, the absence of crystallization during cooling may be due to very characteristic PLA properties, which have a very slow cooling rate during cooling, and/or the cooling rate was too high to allow crystallization in the PLA, particularly in PLA/TPS blend showing a more significant degree of crystallinity. Table 1 shows that the addition of starch to PCL reduces the melting temperature and melting enthalpy of PCL, which may be attributed to reduction of PCL molecular weight and hydrolysis of the ester groups by the water in gelatinized starch, similar to the described work (Su et al. 2012; Averous et al. 2000). The degrees of PCL and PLA crystallinity are 53.6 and 1.4%, respectively. As we can see, PLA is almost completely amorphous with an extremely small fraction of the crystal phase. When they were blended in the same ratio, PCL had a slight decrease in its degree of crystallinity compared to pure PCL, while

Table 1 Summary of the thermal properties of the investigated blends

|	PCL thermal properties						PLA thermal properties					
	T_{gPCL} (°C)	T_{mPCL} (°C)	T_{cPCL} (°C)	ΔH_{cPCL} (J g⁻¹)	ΔH_{mPCL} (J g⁻¹)	λ_{cPCL} (%)	T_{gPLA} (°C)	T_{mPLA} (°C)	T_{ccPLA} (°C)	ΔH_{cPLA} (J g⁻¹)	ΔH_{mPLA} (J g⁻¹)	λ_{cPLA} (%)
PCL	−62.8	58.6	26.9	63.3	70.7	53.6	–	–	–	–	–	–
PLA	–	–	–	–	–	–	56.7	149.4	127.0	1.3	1.3	1.4
PCL/TPS	−61.3	56.1	28.8	40.1	49.4	53.4	–	–	–	–	–	–
PLA/TPS	–	–	–	–	–	–	54.4	147.0	119.4	15.3	15.8	24.1
PCL30/PLA70	–	56.6	30.2	14.4	19.5	49.2	–	149.3	121.1	11.2	11.2	17.1
PCL30/PLA70/TPS	–	56.9	30.1	14.5	14.5	52.0	–	147.6	122.6	8.4	6.6	14.4
PCL50/PLA50	–	51.9	30.2	27.7	33.5	50.8	–	146.0	124.0	3.7	4.1	8.8
PCL50/PLA50/TPS	–	57.4	29.9	17.8	20.8	45.0	–	145.4	117.9	8.0	9.1	27.6
PCL70/PLA30	–	57.1	30.8	41.3	51.6	47.7	–	149.1	120.8	3.2	4.8	17.1
PCL70/PLA30/TPS	–	58.4	30.5	25.5	25.6	39.6	–	146.9	119.0	3.0	4.2	21.3
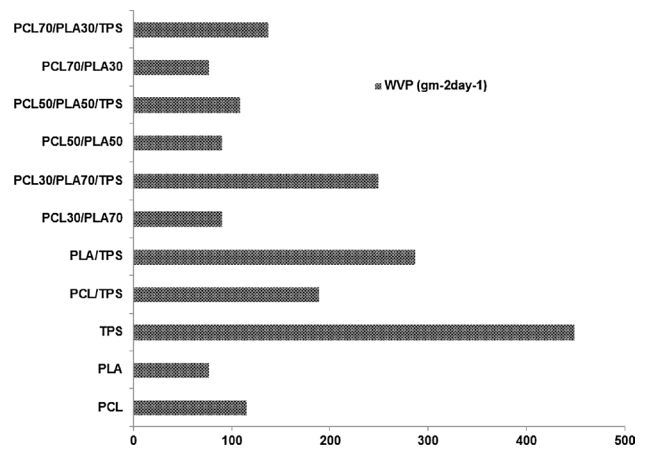
Fig. 5 WVP of the investigated biodegradable blends

PLA became pronouncedly more crystalline. With subsequent addition of TPS to a PCL/PLA (1:1) blend, the same behavior occurred for PCL, as well as for PLA where the degree of PLA crystallinity increased dramatically from 8.8 to 27.6%. Given the degree of crystallinity, it is apparent that both TPS and PLA interfere with the mobility of PCL chains, resulting in a reduction in the degree of PCL crystallinity. When TPS was added to the PCL/PLA blend, it caused an additional increase of the T_{mPCL} in the blends. On the other hand, adding TPS reduced the T_{mPLA} of PLA. These shifts in the melting temperature of PLA or PCL by addition of TPS in the blends may occur due to the distinct amorphous and soluble TPS and PCL fractions that can be miscible in the PLA phase or the soluble TPS and PLA fractions that can be miscible in the PCL phase (Carmona et al. 2015). By increasing the PCL content in ternary blends, the thermoplastic starch disrupted the regularity of the chain structures and thereby increased the free space between chains and as a result T_{mPCL} and χ_{cPCL} were decreased (Davoodi et al. 2016). However, in the PCL/PLA and PCL/PLA/TPS blends, both PCL and TPS enabled further PLA chain mobility, resulting in an increased degree of PLA crystallinity. When TPS is present in polymer blends, the degree of PLA crystallinity is increased. As for PCL crystallization, when both TPS and PLA were present in polymer blends, they restricted the PCL chain mobility and, thus, PCL showed a slightly lower crystallinity than pure PCL.

Water vapor permeability

For greater freshness and shelf life of foods, it is extremely important to avoid or minimize moisture transfer between the food and the surrounding atmosphere. Therefore, as a barrier property, the water vapor permeability is very importance and should be as low as possible to optimize the food

package environment and potentially increase the shelf life of the food product (Ghasemlou et al. 2013; Hosseini et al. 2013). The results of water vapor permeability (WVP) of the studied blends are shown in Fig. 5. As expected, the thermoplastic starch showed the highest water vapor permeability (449.61 g m^{-2} day^{-1}) which is expected due to its hydroscopic nature, whereas the hydrophobic PCL and PLA samples showed the lowest WVP values (Fig. 5). From Fig. 5, it can be seen that PLA, in spite of the low value of crystallinity compared to PCL, has a lower WVP since the T_g of PLA (56.7) is much higher than that of PCL (-62.8). The diffusion coefficient of water in an amorphous or semi-crystalline polymer is related to the molecular dynamics or segmental motions of the amorphous regions of the polymer. Thus, if the temperature of an amorphous polymer–water system is above the glass transition temperature, T_g, motion will be rapid, the free volume increases, and WVP will be high, while the opposite will be true below T_g (Shogren 1997). Crystals in the polymer structure play an important role in inhibiting the transfer of water vapor permeability due to the small cross section and low permeability restricting chain mobility, thus reducing the WVP of the polymers (Zembouai et al. 2013). Also, the increase of WVP can be linked to the two-phase morphology of PCL/TPS and PLA/TPS blends, allowing penetration of moisture through the surface due to cavity formation. From Fig. 5, it is observed that increase in the PCL content has a positive effect on water vapor barrier properties of PCL/PLA binary blends. PCL/PLA blends show intermediate water vapor barrier properties compared to the PCL, PLA polymers, respectively. On the other hand, the value of WVP of PLA increased by addition of 30, 50 and 70 wt% of PCL, respectively. This means that PLA insertion improves PCL barrier properties even at a relatively low rate, due to the increased PLA crystallinity in the PCL/PLA mixtures. Reduction of the WVP with crystallinity can generally be explained in two ways. Higher crystallinity implies higher content of impermeable crystallites within the structure, thereby reducing the amount of the amorphous phase through which the gas molecules can penetrate. Another fact is that the impermeable crystals increase the tortuosity of the transport path. It is known that the gas transport properties of polymer blends are strongly influenced by the tortuosity of the circulating molecule gases. Gas permeation is carried out exclusively in the amorphous phase of polymer blends. In this way, a semi-crystalline polymer consists of an almost impermeable crystal phase dispersed in the permeable amorphous phase. Therefore, any increase in crystallinity leads to a reduction of the gas permeability, due to reduced contribution of the permeable amorphous phase and to increased tortuosity of the diffusion path (Sun et al. 2017). In our case, the relatively good adhesion between PCL domains and the PLA matrix and higher levels of crystallinity of PLA in the blends, as shown in the DSC analysis and followed by SEM analysis, resulted in a longer path length for the diffusion of water vapor molecules and gas, which led to the decrease in the barrier properties of PCL/PLA blends. In the ternary PCL/PLA/TPS blends, incorporation of thermoplastic starch in blends leads to increase in the WVP value due to the hydrophilic starch character. Also, the incorporation of thermoplastic starch in the PCL and PLA blends reduces the intermolecular force between the PCL and PLA, receptively, resulting in enhancing the gaps in the blend structure. This phenomenon was confirmed by the results from SEM (show below). Ternary blends with higher PCL content had lowest WVP due to better integration in the blend, reducing gaps by creating more compact structure, causing lowered WVP. This may also indicate the existence of better intermolecular interactions and a decrease in the mobility of amorphous thermoplastic starch. The low water vapor permeability, i.e., the acceptable level of water resistance of a blend, is one of the particular important properties from a food packaging point of view, especially for high water activity foods or foods that come into contact with high humidity environments during storage and transportation (Rhim et al. 2007). On the other hand, although for the industrial application of biodegradable blends the hydrophobicity of the material is essential, it is also important that to promote biodegradability a certain level of water vapor permeability must be present after use, because the efficiency of the microorganisms is better in a high humidity environment. Therefore, it is important for the good efficiency of biodegradable materials that they must be suitable for both application and biodegradability. By adding starch to the PCL/PLA blend, a certain degree of water absorption is precisely ensured because starch is a water-sensitive polymer. Hydrogen bonds can be formed between water and its hydroxyl groups. Besides lowering the final price of the material, the role of starch also as a nutrient medium for microorganisms will result in faster biodegradation of the blends.

Biodegradability during the composting process

In the composting process, aerobic mesophilic and thermophilic microorganisms are responsible for the biological treatment of biodegradable organic matter. A microbial population consisting mainly of bacteria and fungi consumes biodegradable organic matter, together with oxygen, and produce CO_2, NH_3, water, compost and a lot of heat (Kučić et al. 2013). In the Fig. 6 is it shown a visual appearance of PCL70/PLA30 samples before and after biodegradable. Due to the exothermic process and the release of large amounts of heat, the temperature in the composting mass increases significantly. Therefore, for maintaining the efficiency of the composting process, temperature is one of the most important parameters (Fig. 7). Several
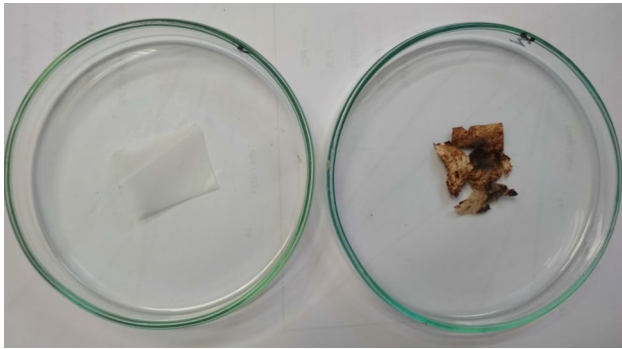
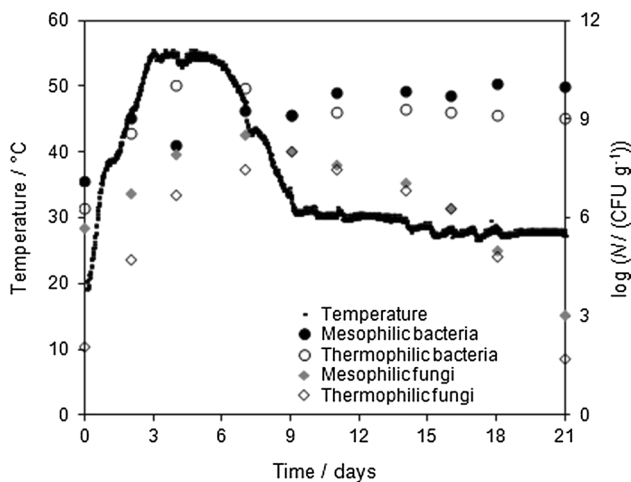**Fig. 6** Visual appearance of PCL70/PLA30 samples before (left) and after (right) biodegradation

Fig. 7 Temperature changes in the composting mass and growth of microorganisms during 21 days of the composting process

Fig. 8 The evolution of carbon dioxide versus temperature during 21 days of the composting process

phases are exchanged during the composting process: mesophilic, thermophilic, cooled (second mesophilic) phase and maturation phase (Fig. 7). Thermophilic phase is the most important for degradation of biodegradable blends, due to the extremely high temperature which favors the degradation of organic matter by microorganisms (Fig. 7). Permanent temperature change in a reactor leads to a change in the microbial species involved in the degradation of the substrates and biodegradable polymers. Also, the rise in temperature in the composting mass favors the growth of thermophilic microorganisms and ultimately affects their activity. According to Jayasekara et al. (2005), a key change in polymer degradation is the decrease in molecular weight due to the formation of smaller products during decomposition. The starch can be degraded by fungi and/or bacteria due to enzymatic activity, leading to the formation of carbon dioxide, water, and sugar (Neto et al. 2017) (Fig. 8). Due to its hydrophilic character, starch degrades firstly and rapidly, thus facilitating access
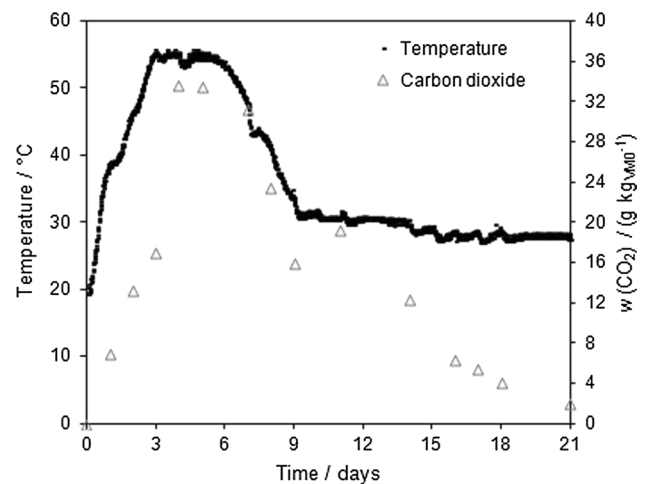
by microorganisms, encouraging the biodegradation of other components in the blend (Neto et al. 2017). During 21 days of the composting process, some samples (PCL, PCL/TPS, PCL50/PLA50, PCL50/PLA50/TPS, PCL70/PLA30 and PCL70/PLA30/70) undergo degradation by microorganisms and some of them lose up to 68% of their initial mass. From Fig. 9a, b, it is apparent that some samples, especially with a higher content of PLA (PLA, TPS, PLA/TPS, PCL30/PLA70 and PCL30/PLA70/TPS), were completely degraded during the 21 days of the composting process, probably associated with a predominantly amorphous structure of the neat PLA and higher value of the WVP, which is a attractive medium for microorganisms (Perotti et al. 2017; Ferri et al. 2016). Microorganisms initially attack and consume at first the wheat starch, leading to fracture the blend structure and then polylactide or polycaprolactone chains, which promote further biodegradation process. The thermoplastic starch is attractive and accessible to microorganisms and promotes the biodegradable procedure. Comparison of the data shown in Fig. 9a indicates that neat PCL exhibits a lower rate of biodegradation due to its crystalline structure (DSC results). In fact, the blends with minor percentage of PCL are more liable to biodegradation than those with a higher percentage of PCL. Therefore, in this study, the slower biodegradation of the blends with higher content of PCL compared to other blends is due to the slow biodegradability of the pure polycaprolactone because of high crystallinity, as well as the hydrophobic molecular structure of the PCL. Additionally, the PCL may also prevent microorganisms from accessing the thermoplastic starch (TPS) phase in the depth of the blend, probably because the hydrophobic chains of polycaprolactone prevents hydrophilic enzymes from accessing the TPS contained in the blend.
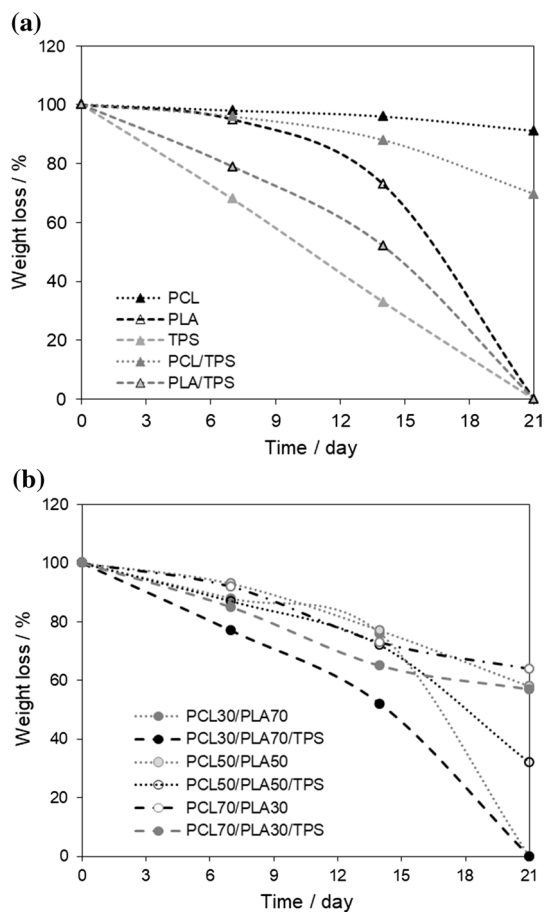
Fig. 9 Weight loss value of the **a** PLA, PCL, TPS and binary PCL/TPS, PLA/TPS blends and **b** binary and ternary blends during the composting process as a function of time

Morphology

The biodegradation of the samples was monitored also by scanning electron microscopy. For the sake of brevity, the

main text shows only selected samples with typical morphological features (Figs. 10, 11) and the complete results are given in the supplementary materials (Figs. S1 and S2). Figure 10 displays the SEM micrographs of the PCL sample with 30 wt% of TPS. Before biodegradation, the surface of the sample was smooth (Fig. 10a) and the small surface asperities came probably from not-perfectly plasticized starch granules. Some amount of non-plasticized starch granules was observed also in the fracture surfaces of all other starch-containing samples (see Fig. 2 and Figs S2 in the Supplementary material). After biodegradation, the surface showed large smooth areas containing holes with quite sharp boundaries (Fig. 10b). The smooth areas were attributed to the slowly degrading PCL matrix, while the sharp holes came from fast degrading TPS minority phase. These results were in good agreement with weight loss experiments, which proved the expected slow biodegradation of PCL that increases after the addition of TPS.

Figure 11 displays the SEM micrographs of the PCL70/PLA30 system, both with and without thermoplastic starch, and both before and after biodegradation. The fracture surface of PCL/PLA sample without thermoplastic starch (Fig. 11a) was smooth, which suggested good interfacial adhesion between the components, as the fracture propagated directly through the whole sample and not along the interface between the two phases. This morphology is typical of compatible polymer blends (Slouf et al. 2004). The material looked quite compact, without voids and inhomogeneities. The small white structures in the middle of the samples were microplastic deformations, which developed due to local overheating during the fracture (Slouf et al. 2004; Fox and Fuller 1971). The fracture surface of the PCL/PLA sample after biodegradation (Fig. 11b) looked less compact and could be attributed to biodegradation-induced changes of both components. The fracture surface of the PCL/PLA system with TPS before biodegradation (Fig. 11c) contained occasional non-plasticized starch granules, whose presence
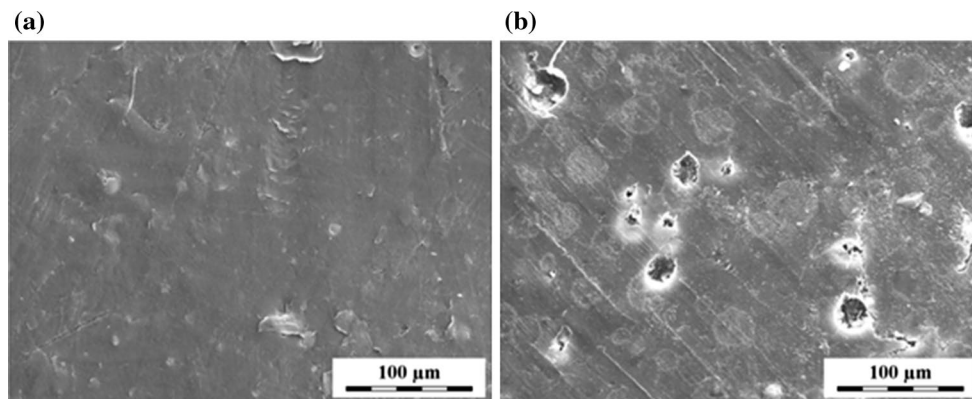

Fig. 10 SEM micrographs showing the top surface of the PCL/TPS sample **a** before and **b** after biodegradation
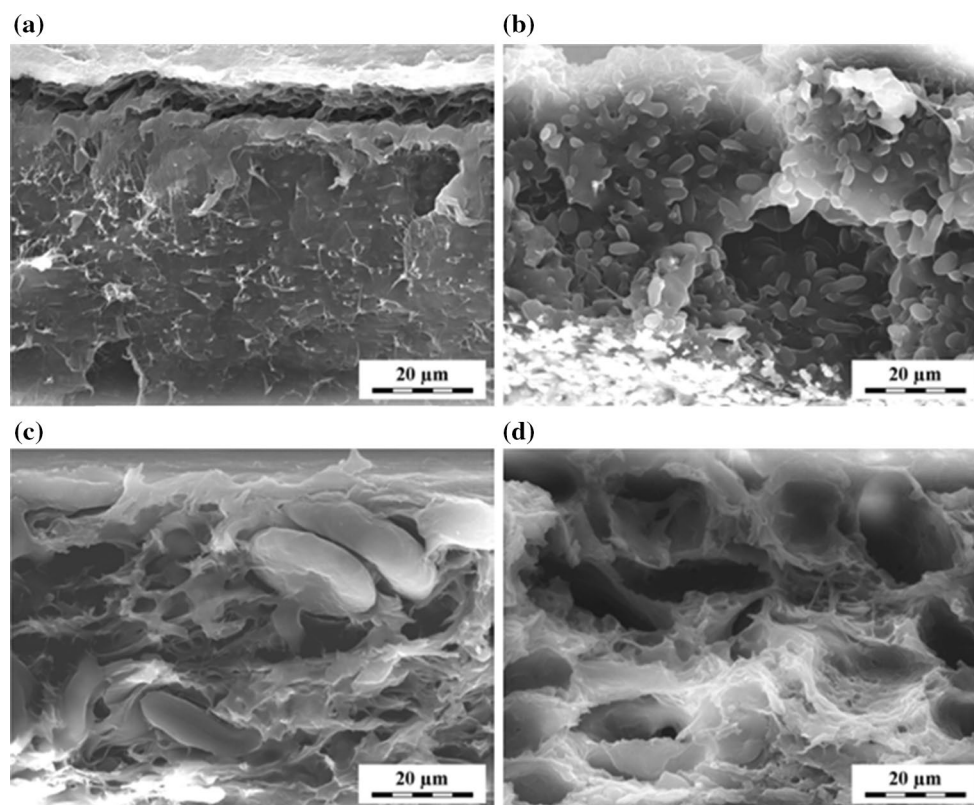
Fig. 11 SEM micrographs showing the fracture surface of blends: **a** PCL70/PLA30 before biodegradation, **b** PCL70/PLA30 after biodegradation, **c** PCL70/PLA30/TPS before biodegradation and **d** PCL70/PLA30/TPS after biodegradation

was detected also on the top surfaces of starch-containing samples (Fig. 10, Fig. S2 in Supplementary material). The interfacial adhesion between starch and the matrix was poorer than the interfacial adhesion between PCL and PLA themselves, as the fracture propagated along the interface of non-plasticized starch granules; the propagation of fracture along the interface of the particles is typical of non-compatible blends (Fortelny et al. 2006). The fracture surface of PCL/PLA blends with TPS after biodegradation exhibited a much higher extent of damage than the blends without starch (compare Fig. 11b and d): firstly, the TPS inclusions were completely degraded; secondly, the PCL/PLA matrix was less compact and showed microscale voids and cracks.

In conclusion, the SEM micrographs clearly evidenced that thermoplastic starch-containing samples degrade faster than analogous samples without thermoplastic starch.

Infrared spectroscopy

The observed differences between the ATR FTIR spectra of the samples measured before and after biodegradation indicate significant changes in the molecular composition (Fig. 12). Relevant changes in the spectra were observed mainly in three regions: intensity decrease of the bands at 1800–1700 cm^{-1} (C=O stretching bands of PCL and PLA) were compensated by the increase of the bands in the region 3400–3200 cm^{-1} (OH stretching) and by several new bands in the region 1700–1500 cm^{-1}. The degree of biodegradation could be estimated from the intensity decrease of the C=O stretching bands assigned to PLA (1758 cm^{-1}) and to PCL (1736 and 1722 cm^{-1} assigned to the amorphous and crystalline phase, respectively). In general, the TPS containing systems degraded faster than corresponding systems without TPS, although we observed some variations due to the local character of ATR measurement. Typical spectra for selected samples are summarized in Fig. 12. In pure PCL (Fig. 12a) only negligible biodegradation was observed, but the degraded sample displayed much higher degree of crystallinity. As expected, a higher degree of biodegradation was observed in PCL/TPS (Fig. 12b). Biodegradation was observed also in the PCL50/PLA50 blends (Fig. 12c) and in PCL50/PLA50/TPS (Fig. 12d), where the overall extent of biodegradation looked similar (this could be attributed to local fluctuations on the sample surfaces), but the changes were clearly detectable (increase in OH stretching bands around 3300 cm^{-1}, changes of the C=O stretching band around 1740 cm^{-1}, and increase in the region below 1700 cm^{-1}, which are discussed below).

(a)

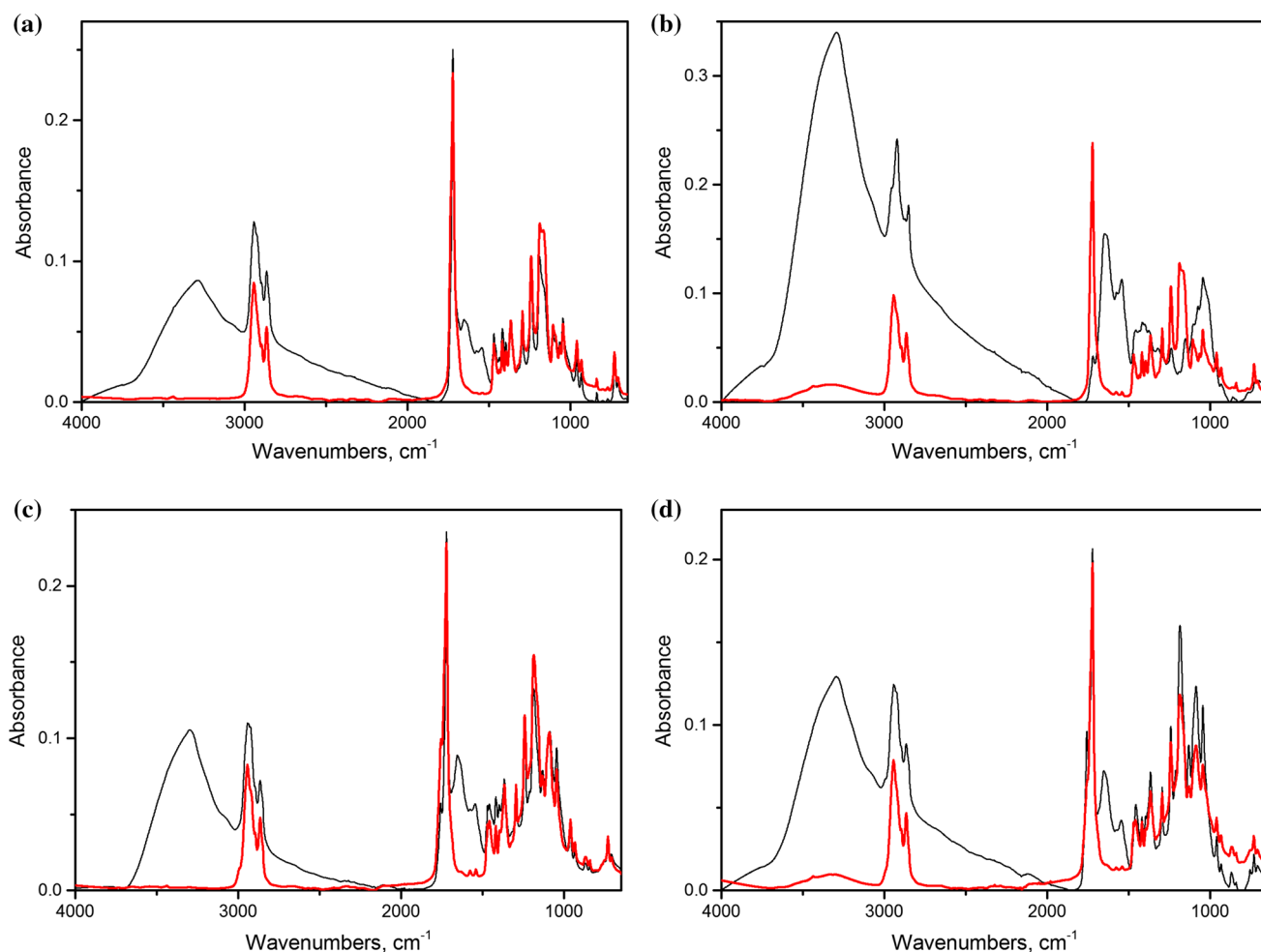**(b)**

(c)

(d)

Fig. 12 FTIR/ATR spectra of the **a** PCL, **b** PCL/TPS, **c** PCL50/PLA50 and **d** PCL50/PLA50/TPS blends. Thick red lines and thin black lines denote sample before and after biodegradation, respectively

The molecular mechanism of the biodegradation is characterized in the FTIR spectra by the presence of strong bands assigned to OH groups and by the new bands observed at 1700–1500 cm^{-1}, which can be assigned to the amide I and amide II vibrations of the amide groups. Detection of the OH and amide groups in the biodegradation products is in agreement with the biodegradation reactions proposed by Plichta et al. 2014.

Conclusion

In this study, binary and ternary blends of PLA, PCL and TPS in different compositions were generated by the melt mixing method and studied for their thermal, morphological and barrier properties. In binary PCL/PLA blends, PCL had a reduction in its crystallinity, while PLA become more crystalline. The same effect occurred on adding thermoplastic starch, indicating that both TPS and PLA hindered

the mobility of the PCL chain, resulting in a reduction in PCL crystallinity. For the barrier properties of the blend films, water vapor permeability decreased with the addition of PCL. Finally, the biodegradability of binary and ternary blends was confirmed with weight loss measurements with exposure time in composting process. Accordingly, the water vapor permeability of aliphatic polyesters/TPS blends increases with the addition of TPS due to degradation of the starch of the molecule through moisture and the hydrophilic nature of starch. TPS accelerates the biodegradability of the blends, since starch is attractive and accessible to microorganisms.

This research emphasized the importance of biodegradable materials based on thermoplastic starch as a new generation of materials with low cost and improved biodegradability. It is important to note that the use of PCL/PLA/TPS blends is extremely important in reducing the environmental impact caused by the indiscriminate use of conventional plastic in packaging, since they are easily integrated into

the composting cycle. However, there are still many disadvantages of such blends and further studies are needed before using such blends as an active packaging for real food products.

Compliance with ethical standards

Conflict of interest On behalf of all authors, the corresponding author states that there is no conflict of interest.

References

Abdul KHPS, Tye YY, Saurabh CK, Leh CP, Lai TK, Chong EWN, Fazita NMR, Mohd HJ, Banerjee A, Syakir MI (2017) Biodegradable polymer films from seaweed polysaccharides: a review on cellulose as a reinforcement material. eXPRESS Polym Lett 11:244–265. https://doi.org/10.3144/expresspolymlett.2017.26

Ačkar Đ, Babić J, Šubarić D, Kopjar M, Miličević B (2010) Isolation of starch from two wheat varieties and their modification with epichlorohydrin. Carbohydr Polym 81:76–82. https://doi.org/10.1016/j.carbpol.2010.01.058

Antosik AK, Wilpiszewska K (2018) Natural composites based on polysaccharide derivatives: preparation and physicochemical properties. Chem Pap 72:3215–3218. https://doi.org/10.1007/s11696-018-0550-3

Auras R, Harte B, Selke SE (2004) An overview of polylactides as packaging materials. Macromol Biosci 4:835–864. https://doi.org/10.1002/mabi.200400043

Austrian Standards Institute (1986) Austrian standard: analytical methods and quality control for waste compost. ÖNORM S 2023, Vienna

Averous L, Moro L, Dole P, Fringant C (2000) Properties of thermoplastic blends: starch-polycaprolactone. Polymer 41:4157–4167. https://doi.org/10.1016/S0032-3861(99)00636-9

Bota J, Lj Kratofil Krehula, Katančić Z, Brozović M, Hrnjak-Murgić Z (2017) Surface characteristics and enhancement of water vapor properties of paperboard coated with polycaprolactone nanocomposites. J Adhes Sci Technol 31:1–21. https://doi.org/10.1080/01694243.2016.1218313

Briški F, Kopčić N, Ćosić I, Kučić D, Vuković M (2012) Biodegradation of tobacco waste by composting: genetic identification of nicotine-degrading bacteria and kinetic analysis of transformations in leachate. Chem Pap 66:1103–1110. https://doi.org/10.2478/s11696-012-0234-3

Brody AL (2005) Commercial uses of active food packaging and modified atmosphere packaging systems. In: Han JH (ed) Innovations in food packaging. Elsevier Science, Oxford, pp 457–474

Broz ME, Vander HDL, Washburn NR (2003) Structure and mechanical properties of poly(D, L-lactic acid)/poly(ϵ-caprolactone) blends. Biomaterials 24:4181–4190. https://doi.org/10.1016/S0142-9612(03)00314-4

Carbonell-Verdu Ferri JM, Dominici F, Boronat T, Sanchez-Nacher L, Balart R, Torre L (2018) Manufacturing and compatibilization of PLA/PBAT binary blends by cottonseed oil-based derivatives. eXPRESS Polym Lett 12:808–823. https://doi.org/10.3144/expresspolymlett.2018.69

Carmona VB, Corrê AC, Marconcini JM, Capparelli Mattoso LH (2015) Properties of a biodegradable ternary blend of thermoplastic starch (TPS), poly(e-caprolactone) (PCL) and poly(lactic acid) (PLA). J Polym Environ 23:83–89. https://doi.org/10.1007/s10924-014-0666-7

Carvalho AJF, Zambon MD, Curvelo AAS, Gandini A (2003) Size exclusion chromatography characterization of thermoplastic starch composites 1. Influence of plasticizer and fibre content. Polym Degrad Stab 79:133–138. https://doi.org/10.1016/S0141-3910(02)00265-3

Chen L, Qiu X, Xie Z, Hong Z, Sun J, Chen X, Jing X (2006) Poly(L-lactide)/starch blends compatibilized with poly(L-lactide)-g-starch copolymer. Carbohydr Polym 65:75–80. https://doi.org/10.1016/j.carbpol.2005.12.029

Crescenzi V, ManziniG Calzolari G, Borri C (1972) Thermodynamics of fusion of poly-β-propiolactone and poly-ϵ-caprolactone. Comparative analysis of the melting of aliphatic polylactone and polyester chains. Eur Polym J 8:449–463. https://doi.org/10.1016/0014-3057(72)90109-7

Curvelo AAS, Carvalho AJF, Agnelli JAM (2001) Thermoplastic starch-cellulosic fibers composites: preliminary results. Carbohydr Polym 45:183–188. https://doi.org/10.1016/S0144-8617(00)00314-3

Davoodi S, Oliaei E, Davachi SM, Hejazi I, Seyfi J, Be S, Ebrahimi H (2016) Preparation and characterization of interface-modified PLA/starch/PCL ternary blends using PLLA/triclosan antibacterial nanoparticles for medical applications. RSC Adv. 6:39870–39882. https://doi.org/10.1039/c6ra07667j

Feng F, Ye L (2011) Morphologies and mechanical properties of polylactide/thermoplastic polyurethane elastomer blends. J Appl Polym Sci 119:2778–2783. https://doi.org/10.1002/app.32863

Ferreira ARV, Alves VD, Coelhoso IM (2016) Polysaccharide-based membranes in food packaging applications. Membranes (Basel) 6:22–39. https://doi.org/10.3390/membranes6020022

Ferri JM, Fenollar O, Jorda-Vilaplana A, García-Sanoguera D, Balart R (2016) Effect of miscibility on mechanical and thermal properties of poly(lactic acid)/polycaprolactone blends. Polym Int 65:453–463. https://doi.org/10.1002/pi.5079

Fortelny I, Slouf M, Sikora A, Hlavata D, Hasova V, Mikesova J, Jacob C (2006) The effect of the architecture and concentration of styrene-butadiene compatibilizers on the morphology of polystyrene/low-density polyethylene blends. J Appl Polym Sci 100:2803–2816. https://doi.org/10.1002/app.23731

Fox PG, Fuller KNG (1971) Thermal mechanism for craze formation in brittle amorphous polymers. Nat Phys Sci 234:13–14. https://doi.org/10.1038/physci234013a0

Garcia-Campo MJ, Quiles-Carrillo L, Masia J, ReigPérez MJ, Montanes N, Balart R (2017) Environmentally friendly compatibilizers from soybean oil for ternary blends of poly(lactic acid)-PLA, poly(epsilon-caprolactone)-PCL and poly(3-hydroxybutyrate)-PHB. Materials 10:1339/1–1339/19. https://doi.org/10.3390/ma10111339

Ghasemlou M, Aliheidari N, Fahmi R, Shojaee-Aliabadi S, Keshavarz B, Cran MJ, Khaksar R (2013) Physical, mechanical and barrier properties of corn starch films incorporated with plant essential oils. Carbohydr Polym 98:1117–1126. https://doi.org/10.1016/j.carbpol.2013.07.026

Gumede TP, Luyt AS, Müller AJ (2018) Review on PCL, PBS, and PCL/PBS blends containing carbon nanotubes. eXPRESS Polym Lett 12:505–529. https://doi.org/10.3144/expresspolymlett.2018.43

Hosseini SF, Rezaei M, Zandi M, Ghavi FF (2013) Preparation and functional properties of fish gelatin–chitosan blend edible films. Food Chem 136:1490–1495. https://doi.org/10.1016/j.foodchem.2012.09.081

Huang SJ (2005) Poly(lactic acid) and copolyesters. In: Bastioli C (ed) Handbook of biodegradable polymers. Rapra Technology Litmited, Shawbury, pp 287–297

Huang M, Yu J, Ma X (2005) Ethanolamine as a novel plasticiser for thermoplastic starch. Polym Degrad Stab 90:501–507. https://doi.org/10.1016/j.polymdegradstab.2005.04.005

Jayasekara R, Harding I, Bowater I, Lonergan G (2005) Biodegradability of a selected range of polymers and polymer blends and standard methods for assessment of biodegradation. J Polym Environ 13:231–251. https://doi.org/10.1007/s10924-005-4758-2

Jiang W, Qiao X, Sun K (2006) Mechanical and thermal properties of thermoplastic acetylated starch/poly(ethylene-*co*-vinyl alcohol) blends. Carbohydr Polym 65:139–143. https://doi.org/10.1016/j.carbpol.2005.12.038

Kolthoff IM, Sandel EB (1951) Inorganic quantitative analysis. Školska knjiga, Zagreb, pp 347–352

Kostakova EK, Meszaros L, Maskova G, Blazkova L, Turcsan T, Lukas D (2017) Crystallinity of electrospun and centrifugal spun polycaprolactone fibers: a comparative study. J Nanomater. https://doi.org/10.1155/2017/8952390

Kučić D, Kopčić N, Briški F (2013) Zeolite and potting soil sorption of CO_2 and NH_3 evolved during co-composting of grape and tobacco waste. Chem Pap 67:1172–1180. https://doi.org/10.2478/s11696-013-0322-z

Labet M, Thielemans W (2009) Synthesis of polycaprolactone: a review. Chem Soc Rev 38:3484–3504. https://doi.org/10.1039/b820162p

Lu X, Zhao J, Yang X, Xiao P (2017) Morphology and properties of biodegradable poly (lactic acid)/poly (butylene adipate-*co*-terephthalate) blends with different viscosity ratio. Polym Test 60:58–67. https://doi.org/10.1016/j.polymertesting.2017.03.008

Mittal V, Akhtar T, Matsko N (2015) Mechanical, thermal, rheological and morphological properties of binary and ternary blends of PLA, TPS and PCL. Macromol Mater Eng 300:423–435. https://doi.org/10.1002/mame.201400332

Musioł M, Sikorska W, Janeczek H, Wałach W, Hercog A, Johnston B, Rydz J, Rydz J (2018) (Bio)degradable polymeric materials for a sustainable future—part 1. Organic recycling of PLA/PBAT blends in the form of prototype packages with long shelf-life. Waste Manag 77:447–454. https://doi.org/10.1016/j.wasman.2018.04.030

Nair LS, Laurencin CT (2007) Biodegradable polymers as biomaterials. Prog Polym Sci 32:762–798. https://doi.org/10.1016/j.progpolymsci.2007.05.017

Neto BAM, Fornari Junior CCM, da Silva EGP, Franco M, Reis NS, Bonomo RCF, de Almeida PF, Pontes KV (2017) Biodegradable thermoplastic starch of peach palm (*Bactris gasipaes* Kunth) fruit: production and characterisation. Int J Food Prop 20:S2429–S2440. https://doi.org/10.1080/10942912.2017.1372472

Ortega-Toro R, Morey I, Talens P, Chiralt A (2015) Active bilayer films of thermoplastic starch and polycaprolactone obtained by compression molding. Carbohydr Polym 127:282–290. https://doi.org/10.1016/j.carbpol.2015.03.080

Palsikowski PA, Kuchnier CN, Pinheiro IF, Morales AR (2018) Biodegradation in soil of PLA/PBAT blends compatibilized with chain extender. J Polym Environ 26:330–334

Perotti GF, Kijchavengkul T, Auras RA, Constantino VRL (2017) Nanocomposites based on cassava starch and chitosan. Modified clay: physico-mechanical properties and biodegradability in simulated compost soil. J Braz Chem Soc 28:649–658. https://doi.org/10.21577/0103-5053.20160213

Plichta A, Lisowska P, Kundys A, Zychewicz A, Debowski M, Florjanczyk Z (2014) Chemical recycling of poly(lactic acid) via controlled degradation with protic (macro)molecules. Polym Degrad Stab 108:288–296. https://doi.org/10.1016/j.polymdegradstab.2014.03.006

Rhim J-W, Lee JH, Ng Perry KW (2007) Mechanical and barrier of biodegradable soy protein isolate-based films coated with polylactic acid. LWT Food Sci Technol 40:232–238. https://doi.org/10.1016/j.lwt.2005.10.002

Sarazin P, Li G, Orts WJ, Favis BD (2008) Binary and ternary blends of polylactide, polycaprolactone and thermoplastic starch. Polymer 49:599–609. https://doi.org/10.1016/j.polymer.2007.11.029

Selke SE (2000) Plastics recycling and biodegradable plastics. In: Harper CA (ed) Modern plastics handbook. McGraw-Hill, New York, pp 12.1–12.108

Selke SE, Culter JD, Hernandez RJ (2004) Plastics packaging: properties, processing, applications, and regulations. Hanser, Cincinnati, pp 448–467

Shogren R (1997) Water vapor permeability of biodegradable polymers. J Environ Polym Degrad 5:91–95. https://doi.org/10.1007/BF02763592

Siracusa V, Rocculi P, Romani S, Rosa MD (2008) Biodegradable polymers for food packaging: a review. Trends Food Sci Technol 19:634–643. https://doi.org/10.1016/j.tifs.2008.07.003

Slouf M, Kolarik J, Fambri L (2004) Phase morphology of PP/COC blends. J Appl Polym Sci 91:253–259. https://doi.org/10.1002/app.13253

Sorrentino A, Gorrasi G, Vittoria V (2007) Potential perspectives of bio-nanocomposites for food packaging applications. Trends Food Sci Technol 18:84–95. https://doi.org/10.1016/j.tifs.2006.09.004

Su J, Chen L, Li L (2012) Characterization of polycaprolactone and starch blends for potential application within the biomaterials field. Afr J Biotechnol 11:694–701. https://doi.org/10.5897/AJB11.251

Sun H, Xiao A, Yu B, Bhat G, Zhu F (2017) Effect of PCL and compatibilizer on the tensile and barrier properties of PLA/PCL films. Polymer (Korea) 4:181–188. https://doi.org/10.7317/pk.2017.41.2.181

Taggort P (2004) Starch as an ingredient: manufacture and applications. In: Eliasson AC (ed) Starch in food: structure, function and applications. Woodhead Publishing Limited, Cambridge, pp 363–392

Thakur VK, Thakur MK (2016) Handbook of sustainable polymers: processing and applications. Pan Stanford Publishing, Singapore

Tumwesigye KS, Oliveira JC, Sousa-Gallagher MJ (2016) New sustainable approach to reduce cassava borne environmental waste and develop biodegradable materials for food packaging applications. Food Packag Shelf Life 7:8–19. https://doi.org/10.1016/j.fpsl.2015.12.001

Vertuccio L, Gorrasi G, Sorrentino A, Vittoria V (2009) Nano clay reinforced PCL/starch blends obtained by high energy ball milling. Carbohydr Polym 75:172–179. https://doi.org/10.1016/j.carbpol.2008.07.020

Yu L, Dean K, Li L (2006) Polymer blends and composites from renewable resources. Prog Polym Sci 31:576–602. https://doi.org/10.1016/j.progpolymsci.2006.03.002

Zembouai I, Kaci M, Bruzaud S, Benhamida A, Corre Y-M, Grohens Y (2013) A study of morphological, thermal, rheological and barrier properties of poly(3-hydroxybutyrate-*co*-3-hydroxyvalerate)/polylactide blends prepared by melt mixing. Polym Test 32:842–851. https://doi.org/10.1016/j.polymertesting.2013.04.004